Book Chapter

Analysis of Diesel Knock for High-Altitude Heavy-Duty Engines Using Optical Rapid Compression Machines

Xiangting Wang[1], Haiqiao Wei[1], Jiaying Pan[1]*, Zhen Hu[1], Xuan Wang[1] and Mingzhang Pan[2]

[1]State Key Laboratory of Engines, Tianjin University, China
[2]School of Mechanical Engineering, Guangxi University, China

***Corresponding Author:** Jiaying Pan, State Key Laboratory of Engines, Tianjin University, Tianjin300072, China

Published **August 18, 2021**

This Book Chapter is a republication of an article published by Jiaying Pan, et al. at Energies in June 2020. (Wang, X.; Wei, H.; Pan, J.; Hu, Z.; Zheng, Z.; Pan, M. Analysis of Diesel Knock for High-Altitude Heavy-Duty Engines Using Optical Rapid Compression Machines. Energies 2020, 13, 3080. https://doi.org/10.3390/en13123080)

How to cite this book chapter: Xiangting Wang, Haiqiao Wei, Jiaying Pan, Zhen Hu, Xuan Wang, Mingzhang Pan. Analysis of Diesel Knock for High-Altitude Heavy-Duty Engines Using Optical Rapid Compression Machines. In: Advances in Energy Research: 3rd Edition. Hyderabad, India: Vide Leaf. 2021.

Acknowledgement: This work was supported by the National Natural Science Foundation of China (52076149, 51825603).

Abstract

In high altitude regions, affected by low pressure and low temperature atmosphere, diesel knock is likely to be encountered in heavy-duty engines operating at low-speed and high-load conditions. Diesel knock is commonly measured through pressure transducers, while there is lack of direct evidence and visualization images, such that its fundamental formation mechanism is still unclear. In this study, optical experiments on the severe diesel knock with destructive pressure oscillations were investigated in an optical rapid compression machine. High-speed direct photography and simultaneous pressure acquisition were synchronically performed, and different injection pressure and ambient pressure conditions were considered. The results show that for the given ambient temperature and pressure, diesel knock becomes prevalent at higher injection pressures where fuel spray impingement is enhanced. For the given injection pressure satisfying spray impingement, knock intensity is increased as ambient pressure is decreased. Further analysis on visualization images shows diesel spray impingement leads to longer ignition delay time, by which near-wall autoignition and supersonic reaction front propagation are induced. Consequently, three distinguishing stages can be observed during diesel knock, i.e. ignition delay, reaction front propagation, and pressure oscillation. Both spray impingement and fuel evaporation processes are considered as the main influencing factors.

Keywords

Diesel Knock; Rapid Compression Machine; Spray Impingement; Auto-Ignition; Reaction Front Propagation

Abbreviations and Nomenclature

T_i	Intake temperature
P_i	Intake pressure
T_c	Target temperature at the TDC
P_c	Target pressure at the TDC
T_w	Cylinder wall temperature

P_{SOI}	Cylinder pressure at the start of injection
FIP	Fuel injection pressure
Δt	Injection pulse width
ΔP_{max}	Knock intensity
t	Time after the TDC

Introduction

According to mega data statistics, more than six million automobiles are operated at high altitude regions around the world [1]. The atmosphere temperature and pressure are relatively low at high altitude regions. Consequently, with the increase of altitude, ignition delay time is longer and burning rate becomes slower, which result in enhanced pressure rise rate in premixed combustion stage and prolonged combustion duration [2,3]. Under low-speed and high-load conditions, severe diesel knock with destructive pressure oscillation is likely to occur in heavy-duty diesel engines. When diesel knock occurs at high altitude regions, its intensity can reach several dozens of atmosphere, which results in cylinder head erosion and piston crown breakdown [4]. However, the detailed mechanism for such an abnormal combustion still remains unclear.

Generally, knock phenomenon in spark-ignition (SI) engines is caused by the end-gas autoignition before the arrival of primary flame [5]. Rudloff *et al*. [6] found that depending on mixture quality and thermodynamic conditions, local autoignition could lead to either deflagration or a transition into detonation. Wang and co-workers [7,8] performed optical experiments in a rapid compression machine (RCM) to explore knock mechanism. They found that with the elevation of thermodynamic conditions, there was a combustion mode transition from sequential autoignition to detonation for end-gas autoignition. Engine knock in diesel engines is generally characterized by excessive noise and vibration due to over-quick pressure rise rate [9]. Several studies have been performed to quantify the characteristics of pressure oscillations through pressure measurements [10-12]. Recently, optical diagnostics as effective tools are also extensively employed to identify the underlying mechanism for diesel knock. Rusly *et al*. [13] performed high-speed imaging of soot luminosity combining with in-cylinder pressure measurement in

an optical diesel engine. They found that flames were observed to oscillate seriously when diesel knock occurred. Zhao *et al*. [14] conducted abnormal combustion experiments in an optical diesel engine. They found that diesel knock involved end-gas autoignition, fast subsonic flame propagation, and strong pressure waves (and even shock waves). However, due to the destructive effect of diesel knock, optical visualizations or fundamental researches are still lack, which limits the clarification of diesel knock formation, especially for the heavy-duty engines operating at high altitude regions.

Currently, advanced fuel injection system and injection strategy are applied in high altitude diesel engines to pursue superior power efficiency and fuel economy [15]. The low ambient conditions and the increasing fuel injection pressure will prolong spray penetration, which leads to a greater possibility of spray impingement [16,17]. Du *et al.* [18] experimentally investigated the effects of injection pressure on combustion characteristics under spray impingement conditions in a constant-volume combustion chamber, and the results showed that impinging spray prolonged ignition delay time at high injection pressures. Amir Khalid and co-workers [19,20] carried out optical experiments within a wide range of ambient conditions and fuel injection pressure. The results showed that the FIP and ambient pressure showed significant influences on fuel evaporation during ignition delay time, which further affected fuel-air premixing process. Spray impingement is considered as potential causes of diesel knock, because attached film combustion and strong pressure oscillations are measured in realistic heavy-duty diesel engines [21]. Jain *et al*. [22] investigated the effects of fuel injection pressure (FIP) on combustion characteristics in a partially premixed charge compression ignition (PCCI) engine. They found that appropriate FIPs promoted combustion due to improved spray atomization. However, further increasing FIP resulted in diesel knock. In conventional diesel engines, longer ignition delay time tends to lead to pressure oscillations owing to rapid localised pressure rise rates in premixed combustion stage [23]. However, fundamental investigations on the effect of the FIP and altitude effects on diesel knock remain scarce when there is obvious spray impingement.

With the above considerations, the primary objectives of this study are to explore the combustion characteristics and underlying reasons of diesel knock for high altitude heavy-duty engines. Optical experiments were reproduced in an optical RCM with well-controlled boundary conditions. The RCM setup can bear extreme conditions and simulate similar conditions of realistic engines. High-speed direct photography and simultaneous pressure acquisition were synchronically performed, and the role of injection pressure and ambient pressure conditions were considered. Visualized images were conducted to understand spray impingement, localized autoignition initiation, and reaction front propagation. The current work can provide useful insights into the control and optimization of combustion processes of heavy-duty diesel engines in high altitude regions.

Experimental Setup and Methodology

Experimental Setup

The current studies were conducted in a newly designed high-strength optical RCM in the State Key Laboratory of Engines (SKLE) at Tianjin University. The schematic of the RCM setup is presented in Figure 1. The RCM setup consists of five major sub-systems, including a compression chamber, a combustion chamber, a pneumatically driven chamber, a hydraulically damped chamber, and a high-pressure air tank. The RCM can bear a maximum pressure as high as 300 atm and reach a target pressure as much as 60 atm at the Top Dead Center (TDC). By adjusting compression stroke and clearance volume, the compression ratio can vary from 10 to 21 to achieve different ambient conditions encountered in realistic diesel engines. Meanwhile, a flat piston with crevice containment concept was deigned to guarantee homogenous environment and avoid roll-up vortices [24]. A high-accuracy motional pickup transducer was equipped to measure the law of piston motion.

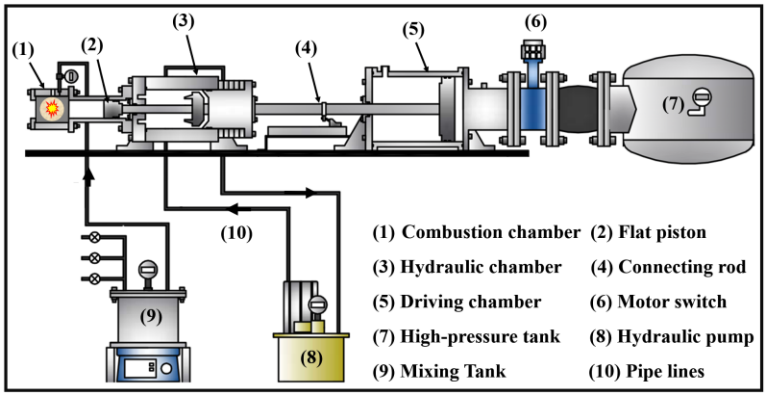

Figure 1: Schematic of high-strength optical rapid compression machine setup.

To understand the pressure characteristics of severe diesel knock, the dynamic pressure trajectories were measured by a piezoelectric pressure transducer (6045A; Kistler). Then the voltage signal was amplified by a charge amplifier (Kistler 5064C), and then was collected by date acquisition equipment (USB 6366, National Instruments) at a frequency of 100 kHz and finally saved to the computer. To visualize the combustion evolution, the combustion chamber was equipped with a high-pressure resistance quartz glasses with the thickness of 40 mm in the axial direction. A high-speed direct camera (Photron SA-Z) with a 105-mm lens (AFMicro Nikkor 1: 2.8 D) was performed to record the combustion images. The camera frame rate can reach a frequency of up to 20 wHz (5 μs/frame) at the resolution of 320 × 128 pixel. The shutter speed was set to 8.39 μs and the lens aperture was maximized to improve definition and underexposure during combustion. At the same time, the camera was synchronously triggered by transient pressure signals with a defined threshold. In addition, a commercial fuel injector with a single hole was edge-installed in the combustion chamber. Figure 2 shows the schematic of the optical combustion chamber with pressure transducer and the fuel injector.

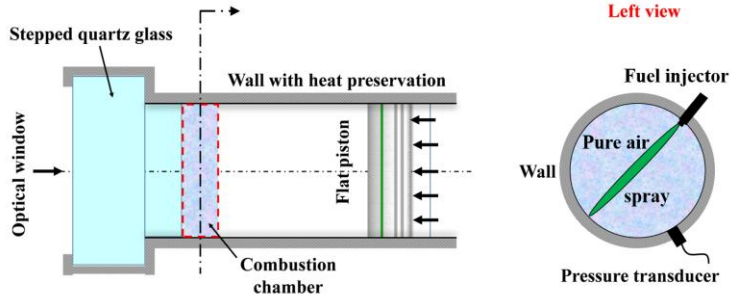

Figure 2: Schematic of optical combustion chamber & fuel injector and pressure transducer layout.

In the experiments, a commercial diesel fuel, was injected by a Bosch single-shot common-rail fuel injection system with the maximum injection pressure up to 140 MPa. The cetane number of diesel fuel used in this research is 42.3 and more detailed properties are revealed in the Table 1. According to the method of SH/T0606-2005 [25], the composition of diesel fuel was analyzed to understand the autoignition characteristics. To accurately control a solenoid force, the injector is controlled by an injector driver box and a LabView VI. Meanwhile, a TTL pulse is employed to control injection timing and pulse width to quantify injected mass in the experiment. Figure 3 shows the calibration of injection mass versus fuel injection pressure. And the injector body is water-cooled to ensure the injector operates normally when the RCM is heated.

Table 1: Fuel properties of the diesel fuel in the experiment.

Diesel fuel	Straight-run diesel
Viscosity (mm^2/s) @ 293K	2.344
Cetane number	42.3
Density(kg/m^3) @ 293K	817.0
Flash point (K)	335.0
Low heating value (MJ/kg)	42.84
Distillation of 50% (K)	518.5
Distillation of 90% (K)	601.4

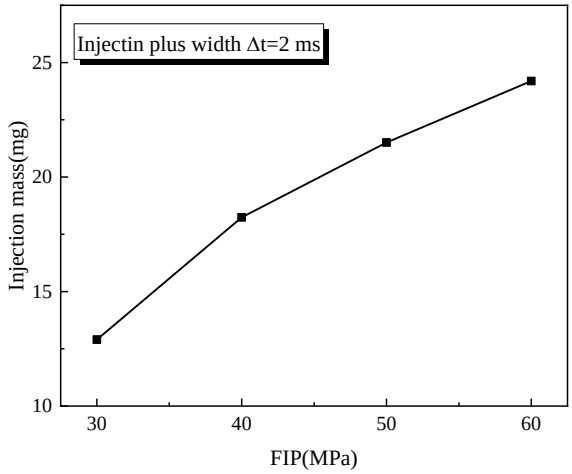

Figure 3: Calibration results of injection mass versus fuel injection pressure.

Test Operation Conditions

In the experiments, ultra-high purity air (>99.999%) consisting of 21% O_2 and 79% N_2 was firstly prepared in a 6.0 L mixing tank to adopted as background gases. The amounts of pure air and fuel mass were calculated at ambient conditions. Meanwhile, the mixing tank was equipped with a magnetic stirring apparatus and it was taken at least 2 hours to improve the mixture homogeneity. An electric heating system involving PID control was used to heat all connection pipelines, and the target temperature was the same as the mixture inside the mixing tank to avoid fuel condensation. To mimic the realistic wall temperature in diesel engines, the wall temperature of the combustion chamber is maintained at 363 K [13]. Besides, experimental data on diesel knock from realistic high-altitude heavy-duty engines have been provided as reference, which can be seen in Supplementary Materials.

Table 2 shows the experimental conditions of the current study. The fuel injection pressure was varied from 30 to 60 MPa to investigate the influence of FIP. The diameter (d) of the single hole injector maintained 0.32 mm to simulate the actual scenarios of heavy-duty diesel engines. The start of injection (SOI) timing was triggered when the instantaneous in-cylinder pressure reached 10 atm to simulate the engine scenarios under

high altitude conditions. However, there is slight difference in injection timing because fuel injector needs certain response time for the signals from microcontrollers. Two groups of injection pulse width were adopted (i.e. Δt=1.5 and 2.0 ms) to consider the effect of injection mass on diesel knock. The respected target pressures at the TDC are P_c=21.4 atm and P_c=41.3 atm, which are similar to the realistic engine scenarios at high altitude regions (e.g. 4500 m) [26]. The intake temperature (T_i) was controlled at 343 K, and the target temperature at the TDC (T_c) was calculated by an adiabatic core hypothesis relation [27]:

$$\int_{T_i}^{T_c} \frac{\gamma}{\gamma\text{-}1} \frac{\mathrm{dT}}{\mathrm{T}} = \ln\left(\frac{P_c}{P_i}\right) \quad (1)$$

where γ is the specific heat ratio which is function of temperature. It is noted that the specific heat ratio of different temperatures has been obtained based on a table checking method. Meanwhile, experiment was repeated at least 3 times at each operating condition to improve the consistency of experimental results. Because spray impingement may result in soot production and deposition, the combustion chamber has to be cleaned after each operating condition to avoid the concerns by soot particles.

Table 2: Test conditions for RCM experiments.

D (mm)	P_i (atm)	T_i (K)	P_c (atm)	T_c(K)	P_{SOI} (atm)	FIP (MPa)	Δt (ms)
70	0.65	343	21.4	930.8 ±5	10	30-60	1.5,2.0
70	1.30	343	41.3	921.4 ±5	10	30-60	1.5,2.0

Figure 4 show the operational stabilities of non-reactive and reactive conditions. It can be clearly that for non-reactive cycles, the pressure trace at different tests shares almost the same trajectories during the whole processes. For the reactive conditions, the compression process shows great repeatability despite there is slight difference in pressure rise when combustion starts. Figure 5 further indicates the diesel knock scenarios under the condition of FIP=60MPa. It is observed that there are still some differences in autoignition onset and the peak of pressure trajectories under abnormal conditions due to the

stochastic nature caused by the in-cylinder temperature inhomogeneities. However, the results given in the Figure5 still show good stability in the compression process. All in all, the current RCM setup shows good repeatability in diesel knock. Besides, it is worth noting that diesel knock intensity (ΔP_{max}) is defined as the maximum amplitude of pressure oscillation obtained from in-cylinder transient pressure using 4-25 kHz bandpass filtering with fast Fourier transformation. Based on previous knocking studies in SI engines [28], the combustion cycles with $\Delta P_{max} > 20$ atm were regarded as super-knock events. Herein, similar method is also employed to distinguish the severe diesel knock.

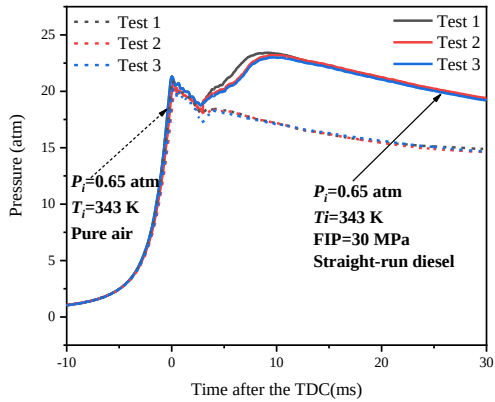

Figure 4: Stability of RCM experiments for pure air compression and normal combustion.

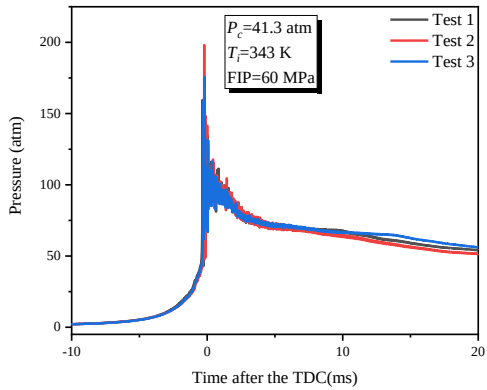

Figure 5: Capability of RCMs in studying diesel knock.

Results and Discussion

Effects of Fuel Injection Pressure

The effects of fuel injection pressure on diesel knock are firstly investigated for two different compressed pressure. As can be seen from Figure 6, the pressure and pressure oscillation curves show different characteristics with varying fuel injection pressure. Specifically, there is no obvious pressure rise under the conditions of FIP=30 MPa, until FIP is increased to 40 MPa where harness combustion is encountered under the conditions of P_c=21.4 atm. However, the maximum pressure is only 64.4 atm. Meanwhile, it should be noted for the conditions of P_c=21.4 atm and FIP =40 MPa, normal combustion with slight pressure oscillation is observed. As fuel injection pressure elevates to 50 MPa, pressure rise rapidly and abnormal combustion begins to happen. Further increasing FIP to 60 MPa, knock intensity is both enhanced under two scenarios. And the peak of pressure oscillations reach ΔP_{max}=79.8 atm (P_c=21.4 atm) and ΔP_{max}=58.5 atm (P_c=41.3 atm), which are manifested super-knock level based on knock criteria aforementioned [4]. Therefore, for the given compressed pressure, diesel knock becomes prevalent with the increase of fuel injection pressure.

The elevated knock intensity may be attributed by the increases of diesel injection mass at higher FIP. More diesel fuel mass results in massive fuel-air mixture formation before premixed combustion, which enhanced the energy release and enlarges the amplitude of pressure oscillations. To further illustrate the influence of diesel injection mass, Figure 7 shows the results of injection plus width at Δt=2 ms. It can be observed that compared with Δt=1.5 ms scenarios, knock intensity becomes more violent with increasing the FIP from 40 to 60 MPa. To be more specific, the strongest knock intensity occurs at FIP=60 MPa, with the peaks of pressure oscillation of ΔP_{max}=94.9 atm at P_c=21.4 atm and ΔP_{max}=64.3 atm at P_c=41.3 atm, respectively.

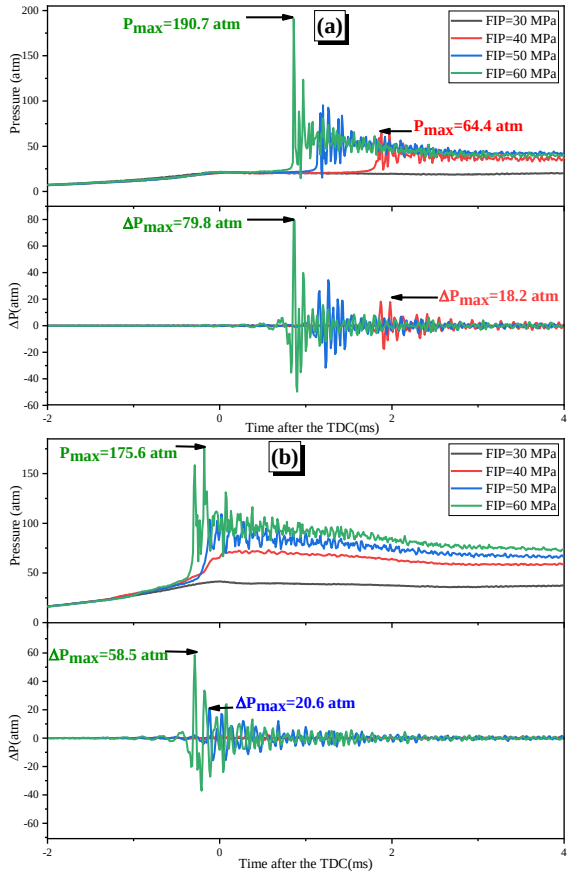

Figure 6: In-cylinder pressure and pressure oscillations at (a)T_c=930.8 K, P_c=21.4 atm, Δt=1.5 ms, (b)T_c=921.4 K, P_c=41.3 atm, Δt=1.5 ms.

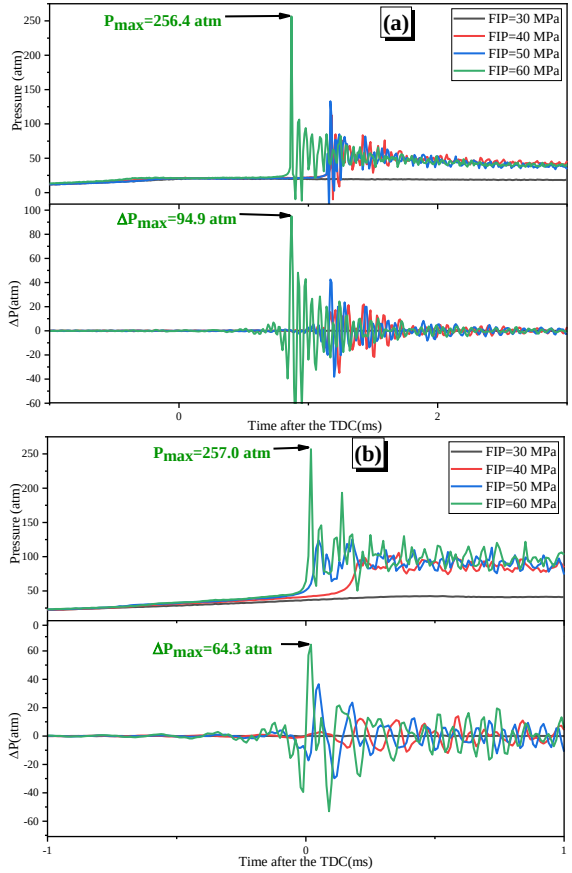

Figure 7: In-cylinder pressure and pressure oscillations at (a) T_c=930.8 K, P_c=21.4 atm, Δt=2.0 ms. (b)T_c=921.4 K, P_c=41.3 atm, Δt=2.0 ms.

To further clarify the effects of FIP, the detail information given in the Figure8 provide insight into spray characteristics and combustion evolution under the conditions of T_c=930.8 K, P_c=21.4 atm, Δt=1.5 ms. First, a small amount of combustible mixture starts to ignite near the injector due to the limited momentum and penetration rate at low injection pressure (FIP=30 MPa). Meanwhile, it is really difficult to form flame kernel and propagate forward owing to the poor atomization process. When elevating injection pressure, the liquid spray begins to impinge the chamber wall with higher penetration rate. However, the impinging fuel cannot ignite immediately due to

the low temperature of wall surface (**T_w**=363 K), which enhances fuel-air mixing process [18]. As can be seen in the Figure8 (B), (C) and (D), an area with blue luminosity occurs at the near-wall region adjacent to the location of spray-wall impingement, and the blue luminosity represents the auto-ignition of vaporized fuel-air mixtures. In addition, the liquid spray impinges against the chamber wall in advance due to the larger momentum at higher FIPs [29], which causes the occurrence of auto-ignition earlier. Higher FIPs also provide a higher upward gas velocity [30], pushing the auto-ignition location farther from the spray-wall impingement region, as shown in Figure8. Finally, the blue reaction wave propagates forward with a higher speed due to more fuel-air mixture formation, which elevates burning rate and shortens combustion duration.

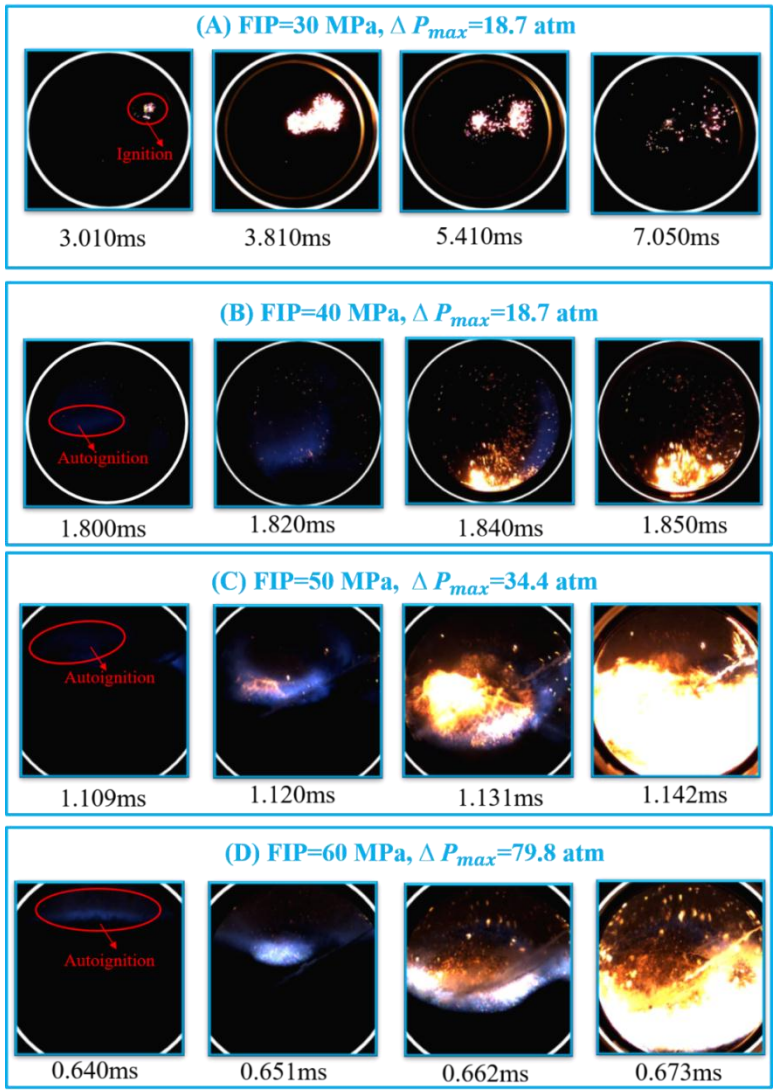

Figure 8: Selected images of combustion evolution under the conditions of T_c=930.8 K, P_c=21.4 atm, Δt=1.5 ms.

Effects of Ambient Pressure

In previous section, there are obviously different pressure characteristics under different compressed pressures with

varying FIPs. Therefore, the effects of ambient pressure are further discussed to investigated the combustion performance for high altitude diesel engine. As shown in Figure 7, knock intensity under low ambient pressure (P_c=21.4 atm) is higher with increasing FIP from 30 to 60 MPa. And increasing injection plus width also enhances diesel knock, which is consistent with the results in previous section. To be more specific, ambient pressure has little influence on combustion performance under the condition of FIP=30 MPa. This can be explained by poor atomization process caused by low fuel injection pressure. However, the impacts of ambient pressure are more pronounced when FIP exceeds 30 MPa, especially for FIP=40 MPa. The results given in Figure 9 show that severe diesel knock is only encountered under the condition of P_c=21.4 atm and Δt=2.0 ms and the knock intensity reaches to ΔP_{max}=34.9 atm. This interesting phenomenon cannot be explained directly. However, in-cylinder pressure traces and visualization images of those conditions could provide insight into the combustion process to deeply clarify the influence of ambient pressure.

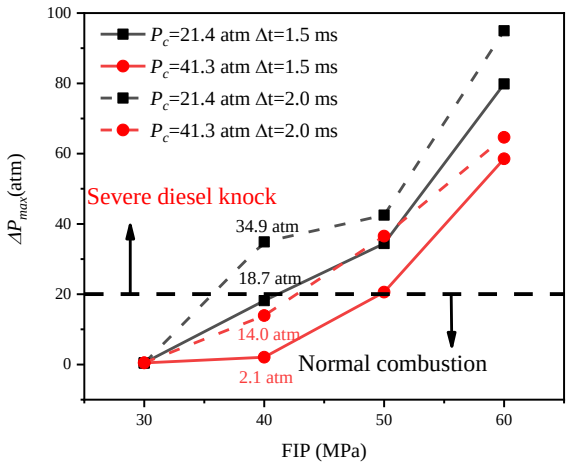

Figure 9: Knock intensity as a function of FIPs at different compressed pressure conditions.

Figure10 (a) firstly shows in-cylinder pressure curves under the conditions of FIP=40 MPa. Despite the cylinder pressure at the start of injection is set at P_{SOI}=10 atm under two scenarios, the

ambient pressure under the conditions of P_c=41.3 atm is higher during the injection duration. Besides, it can be clearly seen that higher ambient pressure leads to shorter ignition delay period and earlier rise of pressure. Generally, evaporation process of spray droplets needs to absorb heat, resulting in a decrease of ambient temperature at spray boundary. However, higher heat capacity caused by higher ambient pressure seems to mitigate the decrease of ambient temperature and increase evaporation rate and fuel-air mixing rate [31]. Therefore, the spray characteristics and mixture formation process may affect this kind of pressure history, which will be discussed later.

The visualization images displayed in the Figure10 (b) further show combustion revolution under two ambient pressure conditions. As seen from the first row, at P_c=21.4 atm, auto-ignition kernel with blue luminosity firstly occurs at the upper corner of the combustion chamber when the time comes to t=1.080 ms after the TDC. At P_c=41,3 atm, a small area of yellow flame appears within the beam of spray at earlier time. This result indicates that the longer ignition delay is a kind of signal that more liquid spray may impinges on the wall under low ambient pressure conditions. From the second column of the images, it is worth mentioning that liquid spray is observed with the help of the higher natural luminescence intensity. It can be concluded that liquid spray is continuously impinging against the wall even after auto-ignition under the conditions of P_c=21.4 atm. However, the spray droplets have been evaporated completely before impinging on the wall when ambient pressure exceeds 40 atm [32]. More combustible mixture is formed locally, and the bright yellow flame is observed near the spray centerline. Then, the flame reaches the wall and ignites the attached fuel film. From the above phenomenon observed in the images, higher ambient pressure weakens liquid spray impingement by accelerating spray evaporation, which further decreases the area and thickness of attached fuel film and knock intensity.

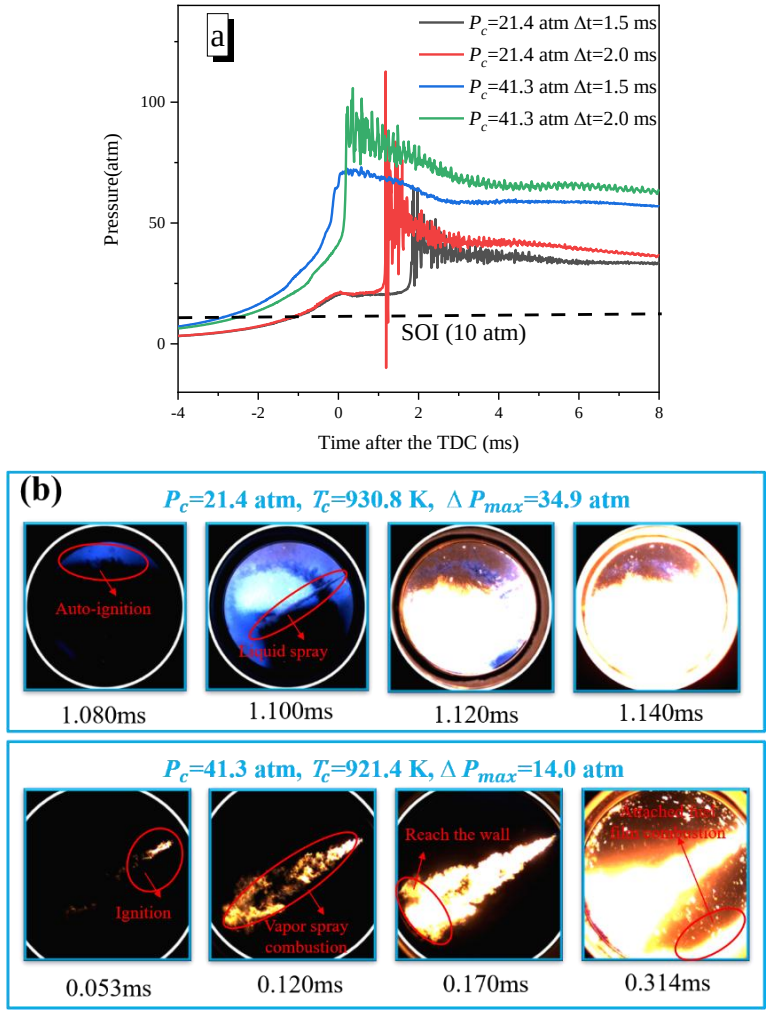

Figure 10: (a) In-cylinder pressure at FIP=40 MPa (b) Selected images of combustion evolution under the conditions of FIP=40 MPa and Δt=2.0 ms.

Analysis of Combustion Evolutions

The effects of fuel injection pressure and ambient pressure on diesel knock have been discussed, however, the underlying reasons for the formation of diesel knock are not clarify. To identify the detailed combustion evolutions of diesel knock, Figure 11 presents typical visualization images at specific

conditions over the pressure traces. Globally, there are three distinguishing stages of the formation process under high altitude scenario, i.e. ignition delay, reaction-front propagation, and pressure oscillation.

The ignition delay time is defined as the time between the start of injection (SOI) and the start of combustion (SOC) [33]. When the fuel does not start to burn, in-cylinder pressure falls slowly owing to heat loss from the combustion chamber boundary. The SOC timing is roughly defined as the moment when in-cylinder pressure begins to rise, as shown in Figure11(A). As can be seen from pressure trace, the ignition delay period is about 1.40 ms due to the spray impingement and low wall temperature, which is very long for tradition diesel engine. A large proportion of fuel-air mixture is prepared within the long ignition delay, which enhances the premixed combustion. Autoignition in end-gas occurs when ignition delay time reaches the threshold. However, the auto-ignition in early phase does not have enough luminosity. Subsequently, a blue reaction front accumulates enough energy and appears in the near-wall region at 1.109 ms after the TDC. This blue reaction front propagates forward and in-cylinder pressure begins to rise rapidly. Then, secondary autoignition by brighter chemiluminescence appears, which induces a secondary reaction-front propagation [34]. As can be seen from Figure 11 (C) and (D), the radius of the secondary reaction-front reaches about 14 mm from 1.120 ms from to 1.131 ms, which indicates an average reaction-front speed of 1272.7 m/s (higher than the local sound speed but lower than the detonation speed at identical operation conditions [35]). Subsequently, this reaction-front reaches the chamber wall, resulting in a correspondingly rapid pressure rise from 30.1 atm to 65.7 atm. When the propagating reaction front collides at the cylinder wall, there is forming an incandescent zone in Figure 11 (E). The reaction-front propagates back and forth in the combustion chamber, which is consistent with the recorded pressure oscillation depicted in the pressure trace.

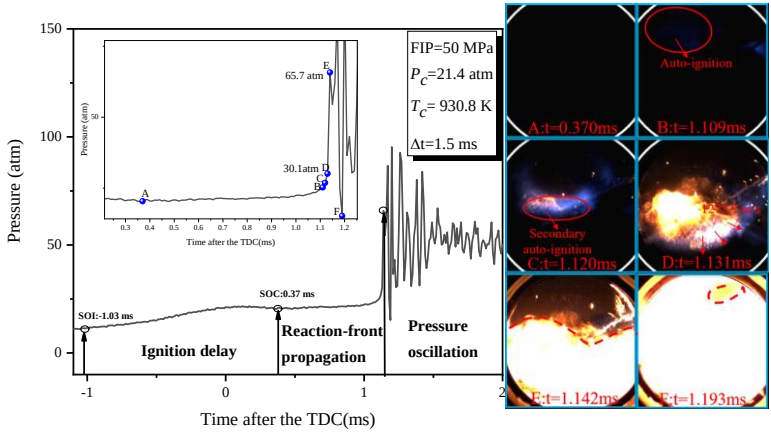

Figure 11: Pressure trace with synchronous images showing three stages of the formation under the conditions of P_c=21.4 atm, FIP=50MPa, Δt=1.5 ms, ΔP_{max}=34.4 atm.

To further clarify the detailed combustion evolutions at more fuel injection mass, Figure 12 shows the typical visualization images and pressure trace under the same condition as injection plus width elevates to 2 ms. It can be clearly seen that there are still three stages during the formation process. The ignition delay time is 1.42 ms in this case, which also indicates that the current RCM setup shows great repeatability. With more injected mass, the area of attached fuel film is enlarged, which accelerates evaporation rate. As a result, a larger area of auto-ignition kernel occurs at earlier time when compared with the previous case. Meanwhile, it should be noted that the reaction-front propagation period is shorter. Based on the locations of the secondary reaction-front in Figure 12 (C) and (D), the speed of this reaction-front is calculated to be about 2054.5 m/s, which means that it is a supersonic detonation speed (C-J detonation speed at D_{cj}=1960 m/s [34]). With the help of the higher natural luminescence intensity of the secondary autoignition, the structure of liquid phrase of spray is observed, indicating that the fuel is still injected into the combustion chamber when secondary autoignition occurs. Continuous fuel-air mixing process elevates mixture energy density, which further accelerates reaction-front speed and enhances knock intensity.

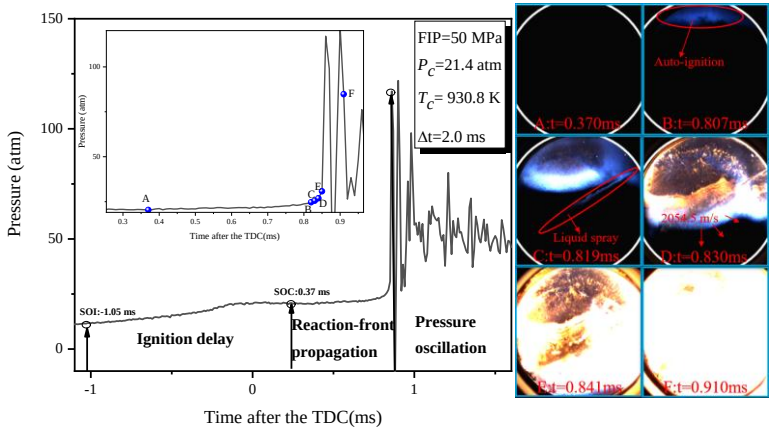

Figure 12: Pressure trace with synchronous images showing three stages of the formation under the conditions of P_c=21.4 atm, FIP=50MPa, Δt=2.0 ms, ΔP_{max}=42.5 atm.

Conclusions

In this study, severe diesel knock with destructive pressure oscillations for high altitude heavy-duty engines was reproduced in a high-strength optical rapid compression machine. High-speed direct photography and simultaneous pressure acquisition were synchronically performed to comparatively investigate the effect of fuel injection pressure and ambient pressure. Typical visualization images were analysed to understand the detailed combustion evolutions during diesel knock.

For given ambient temperature and pressure, diesel knock becomes prevalent with the increase of fuel injection pressure. Possible reasons are that high fuel injection pressure increases injected fuel mass and accelerates the atomization process, which elevates burning rate and shortens combustion duration.

For the given injection pressure satisfying spray impingement, knock intensity is increased as ambient pressure is decreased. This is mainly because higher ambient pressure weakens liquid spray impingement by accelerating spray evaporation, which further decreases the area and thickness of attached fuel film on the wall.

Further analysis on visualization images shows that depending on the long ignition delay induced by diesel spray-wall impingement, severe diesel knock originated from auto-ignition of end gas and supersonic reaction-front propagation. Globally, diesel knock experiences three distinguishing stages: ignition delay, reaction-front propagation, and pressure oscillation.

References

1. Z Kan, Z Hu, D Lou, P Tan, Z Cao, et al. Effects of altitude on combustion and ignition characteristics of speed-up period during cold start in a diesel engine. Energy. 2018; 150: 164-175.
2. X Wang, Y Ge, L Yu, X Feng. Comparison of combustion characteristics and brake thermal efficiency of a heavy-duty diesel engine fueled with diesel and biodiesel at high altitude. Fuel. 2013; 107: 852-858.
3. S Lizhong, S Yungang, Y Wensheng, X Junding. Combustion process of diesel engines at regions with different altitude. SAE. Tech. Paper Ser. 1995.
4. RD Meininger, CBM Kweon, MT Szedlmayer, KQ Dang, NB Jackson, et al. Armstrong, Knock criteria for aviation diesel engines. Int. J. Engine. Res. 2016; 18: 752-762.
5. J Pan, G Shu, P Zhao, H Wei, Z Chen. Interactions of flame propagation, auto-ignition and pressure wave during knocking combustion. Combust. Flame. 2016; 164: 319-328.
6. J Rudloff, JM Zaccardi, S Richard, J Anderlohr. Analysis of pre-ignition in highly charged SI engines: Emphasis on the auto-ignition mode. Proc. Combust. Inst. 2013; 34: 2959-2967.
7. Y Qi, Z Wang, J Wang, X He. Effects of thermodynamic conditions on the end gas combustion mode associated with engine knock. Combust. Flame. 2015; 162: 4119-4128.
8. Z Wang, Y Qi, X He, J Wang, S Shuai, et al. Analysis of pre-ignition to super-knock: Hotspot-induced deflagration to detonation. Fuel. 2015; 144: 222-227.
9. J Heywood. Internal Combustion Engine Fundamentals. New York: McGraw-Hill. 1988.

10. M Syrimis, D Assanis. Knocking cylinder pressure data characteristics in a spark-ignition engine. J. Eng. Gas Turbines Power. 2003; 125: 494-499.
11. Y Ren, R Randall, B Milton. Influence of the resonant frequency on the control of knock in diesel engines. Proceedings of the Institution of Mechanical Engineers, Part D: Journal of Automobile Engineering. London. 1999; 213: 127-133.
12. R Hickling, D Feldmaier, S Sung. Knock-induced cavity resonances in open chamber diesel engines. Acoust. Soc. Am. 1979; 65: 1474-1479.
13. A Rusly, S Kook, E Hawkes, R Zhang. High-speed imaging of soot luminosity and spectral analysis of in-cylinder pressure trace during diesel knock. SAE. Tech. Paper Ser. 2014.
14. M Zhao, S Kaiser. Optical Diagnostics for Knock in Compression-Ignition Engines via High-Speed Imaging. SAE. Int. J. Engines. 2018; 11: 903-918.
15. AK Agarwal, A Dhar, JG Gupta, WI Kim, K Choi, et al. Effect of fuel injection pressure and injection timing of Karanja biodiesel blends on fuel spray, engine performance, emissions and combustion characteristics. Energy. Convers. Manage. 2015; 91: 302-314.
16. F Liu, Z Yang, Y Li, H Wu. Experimental study on the combustion characteristics of impinging diesel spray at low temperature environment. Appl. Therm. Eng. 2019; 148: 1233-1245.
17. AK Agarwal, A Dhar, JG Gupta, WI Kim, CS Lee, et al. Effect of fuel injection pressure and injection timing on spray characteristics and particulate size–number distribution in a biodiesel fuelled common rail direct injection diesel engine, Appl. Energy. 2014; 130: 212-221.
18. W Du, Q Zhang, Z Zhang, J Lou, W Bao. Effects of injection pressure on ignition and combustion characteristics of impinging diesel spray, Appl. Energy. 2018; 226: 1163-1168.
19. A Khalid. Effect of ambient temperature and oxygen concentration on ignition and combustion process of diesel spray. Asian. J. Sci. Res. 2013; 6: 434-444.
20. M Jaat, A Khalid, A Sapit, SM Basharie, AR Andsaler, et al. Effects of temperature and ambient pressure on spray

characteristics of biodiesel combustion, Appl. Mech. Mater. 2015; 773: 501-505.
21. GC Martin, CJ Mueller, DM Milam, MS Radovanovic, CR Gehrke. Early direct-injection, low-temperature combustion of diesel fuel in an optical engine utilizing a 15-hole, dual-row, narrow-included-angle nozzle. SAE. Int. J. Engines. 2009; 1: 1057-1082.
22. A Jain, AP Singh, AK Agarwal. Effect of fuel injection parameters on combustion stability and emissions of a mineral diesel fueled partially premixed charge compression ignition (PCCI) engine. Appl. Energy. 2017; 190: 658-669.
23. P Kyrtatos, K Hoyer, P Obrecht, K Boulouchos. Apparent effects of in-cylinder pressure oscillations and cycle-to-cycle variability on heat release rate and soot concentration under long ignition delay conditions in diesel engines. Int. J. Engine. Res. 2014; 15: 325-337.
24. G Mittal, A Bhari. A rapid compression machine with crevice containment, Combust. Flame. 2013; 160: 2975-2981.
25. L Yu, Y Mao, Y Qiu, S Wang, H Li, et al. Experimental and modeling study of the autoignition characteristics of commercial diesel under engine-relevant conditions. Pro. Combust. Inst. 2019; 37: 4805-4812.
26. BW Weber, CJ Sung, MW Renfro. On the uncertainty of temperature estimation in a rapid compression machine. Combust. Flame. 2015; 162: 2518-2528.
27. Z Wang, H Liu, T Song, Y Qi, X He, et al. Relationship between super-knock and pre-ignition. Int. J. Engine. Res. 2015; 16: 166-180.
28. Z Shi, Cf Lee, H Wu, H Li, Y Wu, et al. Effect of injection pressure on the impinging spray and ignition characteristics of the heavy-duty diesel engine under low-temperature conditions. Appl. Energy. 2020; 262: 114552.
29. A Mohammadi, Y Kidoguchi, K Miwa. Effect of injection parameters and wall-impingement on atomization and gas entrainment processes in diesel sprays. SAE. 2002; 1070-1079.
30. A Khalid, T Yatsufusa, T Miyamoto, J Kawakami, Y Kidoguchi. Analysis of relation between mixture formation during ignition delay period and burning process in diesel combustion. SAE. Tech. Paper Ser. 2009.

31. B Chen, L Feng, Y Wang, T Ma, H Liu, et al. Spray and flame characteristics of wall-impinging diesel fuel spray at different wall temperatures and ambient pressures in a constant volume combustion vessel. Fuel. 2019; 235: 416-425.
32. A Dhole, R Yarasu, D Lata. Investigations on the combustion duration and ignition delay period of a dual fuel diesel engine with hydrogen and producer gas as secondary fuels. Appl. Therm. Eng. 2016; 107: 524-532.
33. J Pan, Z Hu, H Wei, M Pan, X Liang, et al. Understanding strong knocking mechanism through high-strength optical rapid compression machines. Combust. Flame. 2019; 202: 1-15.
34. XJ Gu, DR Emerson, D Bradley. Modes of reaction front propagation from hot spots. Combust. Flame. 2003; 133: 63-74.